

GSA Data Repository 2016273

Development of cutoff-related knickpoints during early evolution of submarine channels

Zoltán Sylvester and Jacob A. Covault

Supplementary material

Movie DR1

Movie DR2

Description of numerical model

The Howard and Knutson (1984) model was implemented using the open-source Jupyter / IPython Notebook computing platform (Pérez and Granger, 2007), with scripts written in the Python programming language.

The HK model is based on the calculation of an adjusted channel migration rate R_1 from a nominal migration rate R_0 , using a weighting function $G(\xi)$:

$$R_1(s) = \Omega R_0(s) + \left[\Gamma \int_0^\infty R_0(s - \xi) G(\xi) d\xi \right] \left[\int_0^\infty G(\xi) d\xi \right]^{-1} \quad (1),$$

where $R_0(s)$ and $R_0(s - \xi)$ are the nominal migration rates at locations s and at a distance ξ upstream from s , respectively. Ω and Γ are weighting parameters that are set to -1 and 2.5 respectively, to produce one of the two parameterizations of stable meandering (Howard and Knutson, 1984). $G(\xi)$ is a weighting function that decreases exponentially in the upstream direction:

$$G(\xi) = e^{-\alpha\xi} \quad (2)$$

The value of the parameter α determines how fast the upstream influence declines; and it is calculated as

$$\alpha = 2kC_f/D \quad (3),$$

where k is a scaling parameter of the order of unity for rivers, D is channel depth, and C_f is the coefficient of friction (Howard and Knutson, 1984). In theory, one could estimate the values of k and C_f for submarine channels and use these to calculate the parameter α . However, using $k = 1$ (Howard and Knutson, 1984) and $C_f = 0.005$, a value commonly used for turbidity currents (Komar, 1975; Pirmez and Imran, 2003; Konsoer et al., 2013), with reasonable values for channel depth, gives relatively small values of α that translate into a slowly decreasing weighting function and a far-reaching upstream influence. This in turn results in a characteristic wavelength that is significantly larger than what is expected in the case of rivers and submarine channels. Therefore, we have tuned the parameters in equation (3) so that the wavelength-width relationship is similar to what has been documented in nature (e.g., Pirmez and Imran, 2003). A comparable approach – tuning the parameters so that the desired wavelength is obtained – has been adopted by Finnegan and Dietrich (2011) as well.

The nominal and actual migration rates are computed from curvature, which in turn is calculated from the Cartesian coordinates of the channel centerline:

$$\eta = \frac{x'y'' - y'x''}{(x'^2 + y'^2)^{3/2}} \quad (4),$$

where x' and x'' denote first and second derivatives of the x coordinate. To model the dependence of migration rate on curvature, we have adopted the functions used by Finnegan and Dietrich (2011):

$$R/W \leq C^*, R_0 = k_l R/W \quad (5),$$

$$R/W > C^*, R_0 = k_l C^{*2} W/R \quad (6),$$

where R is radius of curvature, W is channel width, C^* is a critical value of R/W (which equals $1/\eta W$, that is, the inverse of the dimensionless curvature), and k_l is the lateral migration rate constant. We have used $C^* = 2.0$; this is different from the 5.0 value used by Finnegan and Dietrich (2011), but reasonable taking into account that the resulting actual migration rates match relatively well the river data of Nanson and Hickin (1986) (Fig. DR1), and the resulting channel bend shapes are similar to those observed in the seismic data.

We used a lateral erosion rate constant of $k_l = 3.17 \times 10^{-8}$ m/s (or ~ 2 m/year). This results in actual migration rates of up to 2.7 m/year. These values are relatively large, but not uncommon in rivers (e.g., Nanson and Hickin, 1986; Constantine et al., 2014); and the few observations from modern submarine channels and canyons suggest that such high lateral migration rates may be characteristic of active deepwater systems (Conway et al., 2012; Biscara et al., 2013).

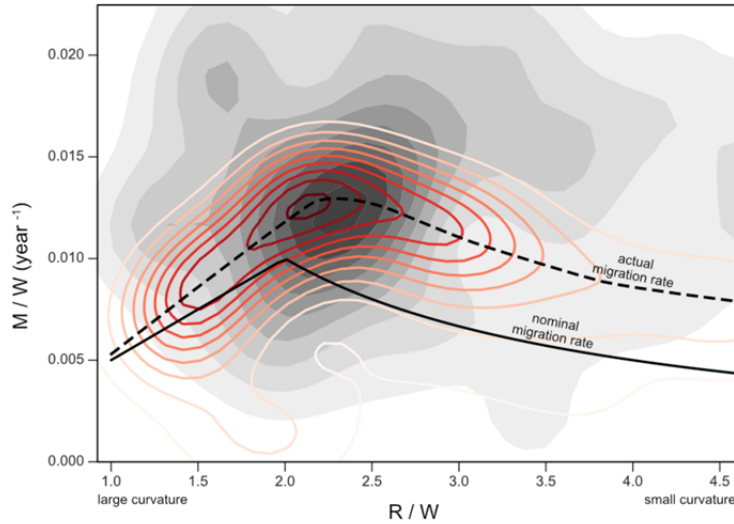


Figure DR1. Plot of nominal (continuous line) and actual (dashed line and red density contours) normalized migration rates (M/W) against R/W , computed for one channel centerline in the HK model, with $k_l = 1.59 \times 10^{-8}$ m/s. River data points ($n = 191$) from Nanson and Hickin (1986) are shown as grey density map in background.

For modeling vertical incision, we use the simplest erosion law that relates vertical incision rate to mean shear stress acting on the channel thalweg (Finnegan and Dietrich, 2011):

$$v = k_v \tau_b \quad (7),$$

where τ_b is the bed shear stress and k_v is a vertical erosion rate constant. For turbidity currents in a submarine channel, the driving force for a volume of fluid of length L is

$$F = \rho R C L g A S \quad (8),$$

where ρ is density of seawater, R is the excess sediment density, C is flow concentration, A is the cross sectional area of the flow, and S is slope (e.g., Konsoer et al., 2013). In the case of steady

and uniform flow the shear stresses on the bottom and top of the current balance this force; assuming that channel depth is small compared to channel width, this balance can be written as

$$\tau_b + \tau_i = \rho RCgDS \quad (9),$$

where D is flow depth and τ_i is the shear stress at the top of the flow. Using $\tau_i = r\tau_b$, we get

$$v = k_v \rho RCgDS / (1 + r) \quad (10).$$

Assuming a sediment concentration of 0.01 and an r value of 0.5 (e.g., Komar, 1975), we find that a vertical slope-dependent erosion rate constant of $k_v = 3.76 \times 10^{-10} \text{ Pa}^{-1} \text{ m}^1 \text{ s}^{-1}$ translates to ~ 0.42 m/year erosion for the initial slope of 0.036. Because the channel slope decreases as sinuosity develops, this relatively large value drops to ~ 0.1 m/year for typical slopes that characterize the sinuous channels in the model. At knickpoint locations slopes are steeper and the rate of incision can be as high as 1.5 m/year. Overall, the incision rates in the model are about an order of magnitude smaller than the lateral migration rates. These values are highly speculative, as data on typical turbidity current concentrations and incision rates is extremely limited. For example, it is possible that erosion is a nonlinear function of slope and it only takes place at quickly migrating knickpoints.

We also need to consider that turbidity currents in submarine channels only last for a few hours or days; therefore, these estimates for erosion rates and shear stresses are long-term averages and erosion rates during individual events must be one or two orders of magnitude larger. Repeat bathymetric surveys of active systems suggest that channel erosion can be surprisingly extensive and fast and these long-term and short-term incision rates are not unreasonable (Conway et al., 2012; Biscara et al., 2013). Furthermore, the overall morphology and stratigraphy of the modeled channel system does not depend on the exact values of the erosion rates; instead, they are driven by the relative magnitudes of the lateral and vertical rates of movement.

For the model illustrated here, we used a channel width of 100 m, channel depth of 5 m, and time step of 12.6×10^6 s (145.8 days). We saved every 100th resulting channel centerline. The initial distance between the points that define the channel was set to 50 m; this distance was kept approximately constant during the simulation by resampling using a parametric spline representation of the curve (Güneralp and Rhoads, 2008). Centerlines were smoothed using a Savitzky-Golay filter (Savitzky and Golay, 1964) in every time step. The initial gradient was set

to 36 m/km, similar to the value estimated for the West Africa example. The meander cutoff threshold was set to three times the channel width; however, a cutoff bend distance of two channel widths gives realistic looking results as well. Although not much is known about the dynamics of cutoffs in submarine channels, the shapes of the cutoff bends in the seismic data used here and in other data volumes (e.g., Deptuck et al., 2007) suggest that cutoff formation can take place at relatively large distances between channel bends. Early cutoff formation in submarine channels could be related to times when the channel undergoes significant filling so that its relief is less prominent ('pseudo meander cutoffs', Deptuck et al., 2007). On the other hand, the incipient cutoff on the Amazon Channel (Fig. 3c) suggests that neck cutoffs with cutoff distances close to one channel width can develop as well.

References

- Biscara, L., Mulder, T., Hanquiez, V., Marieu, V., Crespin, J.-P., Braccini, E., and Garlan, T., 2013, Morphological evolution of Cap Lopez Canyon (Gabon): Illustration of lateral migration processes of a submarine canyon: *Marine Geology*, v. 340, p. 49–56, doi: 10.1016/j.margeo.2013.04.014.
- Constantine, J.A., Dunne, T., Ahmed, J., Legleiter, C., and Lazarus, E.D., 2014, Sediment supply as a driver of river meandering and floodplain evolution in the Amazon Basin: *Nature Geoscience*, v. 7, no. 12, p. 899–903, doi: 10.1038/ngeo2282.
- Conway, K.W., Barrie, J.V., Picard, K., and Bornhold, B.D., 2012, Submarine channel evolution: active channels in fjords, British Columbia, Canada: *Geo-Marine Letters*, v. 32, p. 301–312, doi: 10.1007/s00367-012-0280-4.
- Deptuck, M.E., Sylvester, Z., Pirmez, C., and O Byrne, C., 2007, Migration-aggradation history and 3-D seismic geomorphology of submarine channels in the Pleistocene Benin-major Canyon, western Niger Delta slope: *Marine and Petroleum Geology*, v. 24, no. 6-9, p. 406–433.
- Finnegan, N.J., and Dietrich, W.E., 2011, Episodic bedrock strath terrace formation due to meander migration and cutoff: *Geology*, v. 39, no. 2, p. 143–146, doi: 10.1130/G31716.1.
- Güneralp, I., and Rhoads, B.L., 2008, Continuous Characterization of the Planform Geometry and Curvature of Meandering Rivers: *Geographical Analysis*, v. 40, no. 1, p. 1–25.

- Howard, A.D., and Knutson, T., 1984, Sufficient Conditions for River Meandering: A Simulation Approach: *Water Resources Research*, v. 20, no. 11, p. 1659–1667.
- Komar, P.D., 1975, Supercritical flow in density currents; discussion and reply: *Journal of Sedimentary Research*, v. 45, no. 3, p. 747–753, doi: 10.1306/212f6e33-2b24-11d7-8648000102c1865d.
- Konsoer, K., Zinger, J., and Parker, G., 2013, Bankfull hydraulic geometry of submarine channels created by turbidity currents: Relations between bankfull channel characteristics and formative flow discharge: *Journal of Geophysical Research-Earth Surface*, v. 118, no. 1, p. 216–228, doi: 10.1029/2012JF002422.
- Nanson, G.C., and Hickin, E.J., 1986, A statistical analysis of bank erosion and channel migration in western Canada: *Geological Society of America Bulletin*, v. 97, no. 4, p. 497–504.
- Pérez, F., and Granger, B.E., 2007, IPython: A System for Interactive Scientific Computing: *Computing in Science & Engineering*, v. 9, no. 3, p. 21–29, doi: 10.1109/MCSE.2007.53.
- Pirmez, C., and Imran, J., 2003, Reconstruction of turbidity currents in Amazon Channel: v. 20, no. 6-8, p. 823–849.
- Savitzky, A., and Golay, M.J.E., 1964, Smoothing and Differentiation of Data by Simplified Least Squares Procedures, *Analytical Chemistry* 36 (8), p. 1627-1639, doi: 10.1021/ac60214a047.